doi.org/10.1002/batt.202000048

Optimisation of Formation and Conditioning Protocols for Lithium-Ion Electric Vehicle Batteries

Irene Rubio Lopez,[b] Michael J. Lain,*[a] and Emma Kendrick[b, c]

The formation process and subsequent conditioning (cell ageing) protocols for a commercial EV lithium-ion cell chemistry have been studied to understand their effect on the electrochemical performance and chemical interface. The temperature and duration were varied for both the formation and conditioning steps, and the state of charge was investigated for the conditioning step. The optimum conditioning temperature was shown to be dependent on the previous formation conditions. After formation at room temperature, a longer cycle life was observed when conditioning was performed at 5 °C. After formation at 5 °C, conditioning at 45 °C gave the best cycle life. These results show that the conditioning process is important for cell longevity, and is dependent upon the initial formation. The formation process creates an initial interface layer from reduction of the electrolyte, which rearranges chemically during conditioning. The rearrangement has been followed though impedance studies and XPS analysis. After conditioning at 45 °C, surface analysis of the graphite showed increased quantities of boron and phosphorus in the interface layer, and the fluorine content increased by 20% during the conditioning process. For low temperature formation, greater levels of lithium and oxygen were observed, which subsequently decreased during conditioning.

1. Introduction

The filling, formation and conditioning steps are a very important part of lithium-ion cell manufacture. They have a significant impact on the performance and operating life of the cells. At the end of the conditioning period, any defective cells can be screened out, and some manufacturers will also grade their cells e.g. on capacity. This helps to minimise variability during subsequent usage. All cell manufacturers will have optimised these three steps, as part of their overall cell development programme. However, there are relatively few scientific studies in this area.[1–9] It is important to differentiate between the conditioning stage that occurs during cell manufacture, and the ageing processes that transpire during the operating life of the cell. In cell manufacturing, the conditioning step is called "ageing". Here, we use the name conditioning, to avoid confusion with ageing during the operating life of the cell. Conditioning has a net benefit, unlike the degradation reactions that contribute to cycle ageing or calendar ageing. The most important reaction during formation and conditioning is the creation and stabilisation of the solid-electrolyte interphase (SEI), particularly on the anode. There are many research papers on SEI formation, and several excellent reviews.[1,10–13] Generally, the emphasis is on SEI layer composition and morphology, typically as a function of electrolyte type and electrode surface structure. There has been previous work that correlates the SEI formation conditions to the subsequent cell performance. The SEI layer is characterised after formation, and the effect on cycle life is determined through electrochemical testing.[1–9] In this study, we trace the composition of the SEI layer through conditioning, and elucidate its effect on performance.

It has been reported that formation at high rates produces a porous SEI layer with high electronic conductivity, whereas using low rates gives a dense SEI layer with low electronic conductivity.[1] The effect of formation temperature is more variable, and may depend on the specific cell chemistry. For example, NMC-111/graphite pouch cells were formed using three different protocols, and then charged before storage at 60 °C for ten weeks.[2] The reversible capacity loss was around 15% in each case, but the irreversible capacity loss dropped from 18.4% for formation at 25 °C to 10.5% for formation at 45 °C. The irreversible loss for higher rate formation at 45 °C was 12.8%. In contrast, different NMC-111/graphite pouch cells were formed at four different temperatures, and then cycled at ±3 C.[3] The capacity retention was 15 °C > 25 °C > 35 °C > 45 °C, with the main benefit at the anode. Forming to different voltages (and hence states of charge) had an impact, but this was reversible, and disappeared in subsequent cycling. Protocols with different currents have also been investigated on $LiCoO_2$/graphite cells.[4] A one hour charge at C/10, followed by a CC-CV charge at C, halved the overall formation time, with no compromise on cycling performance.

Studies with a slightly unusual three – five full formation cycles on NMC-532/graphite pouch cells showed some benefits

[a] *Dr. M. J. Lain*
WMG
University of Warwick
Coventry, CV4 7AL, U.K.
E-mail: m.j.lain@warwick.ac.uk
[b] *I. Rubio Lopez, Prof. E. Kendrick*
WMG
University of Warwick
Coventry, CV4 7AL, U.K.
[c] *Prof. E. Kendrick*
School of Metallurgy & Materials
University of Birmingham
Birmingham, B15 2TT, U.K.

Supporting information for this article is available on the WWW under https://doi.org/10.1002/batt.202000048

in only cycling in the upper voltage range.[5,6] The faster protocols led to lower initial cell capacities, but the differences disappeared over 300 cycles. Of greater concern is that the SEI layer may only be "partially built" at the end of formation. This could lead to a less accurate screening test, to remove defective cells. However, "active ageing", in which the cells are cycled between different voltage limits during the normally passive conditioning step, can improve cycle life for NMC-111/graphite cells.[7] The best results were achieved for cells cycled between 3.65 V and 4.0 V.

Cells containing NMC-811 cathodes and graphite anodes were subjected to five different formation protocols, ranging from one cycle at ±C/2 (10 hours) to four ±C/10 cycles (86 hours).[8] The cells were then cycled 300 times, with impedance measurements before and after cycling. The best capacity retention and smallest resistance increase was for cells with intermediate formation protocols (26 or 30 hours). Better electrochemical performance correlated with thinner SEI layers, as adduced from XPS sputter depth profile measurements.

Various accelerated formation protocols were investigated in graphite anode half cells.[9] There were some encouraging signs, but the delithiation capacities on cycling for the standard and novel protocols all appeared to be within the same error bar spread.

The SEI layer has been reported to be formed initially via electrochemical decomposition reactions, as the anode voltage drops from ~3 V vs. Li/Li^+ to just above 0 V vs. Li/Li^+. The SEI layer is extremely complicated, and various spectroscopic studies have identified many components.[12–14] The SEI is usually considered to be a heterogeneous mosaic of different organic, organo-metallic and inorganic phases. Different products are formed as the anode voltage decreases. The initial, loosely bound polymeric organic compounds are supplanted by more compact inorganic compounds.[15] Table 1 lists some of the reaction mechanism that contribute to the SEI layer. The main inorganic components are lithium fluoride and lithium carbonate. Organic phases include polyolefins, and if vinylene carbonate is present in the electrolyte, poly (VC).

The organo-metallic components include lithium alkoxides, and other products from electrolyte dimerization. A recent spectroscopic investigation suggests that the major organo-metallic product is actually LEMC (lithium ethylene monocarbonate, LiO.CO.O.CH_2.CH_2.OH) rather than the more commonly postulated LEDC (lithium ethylene dicarbonate, LiO.CO.O.CH_2.CH_2.O.CO.OLi).[17] There are at least three possible reaction pathways that produce LEMC. LEMC can react further to produce various oligo-carbonates, and related compounds.[18]

Several of these SEI components can be decomposed by HF. They may also dissolve and re-precipitate during conditioning. Thus, the SEI layer is dynamic during conditioning and cycling, and there are also differences between the charged and discharged state.[16] For example, LEMC can react with DMC to produce LMC (lithium methyl carbonate, LiO.CO.O.CH_3), along with ethylene carbonate and methanol.[17]

Several of the reactions produce gaseous by-products, which are extracted from pouch cells during the de-gassing step. Something like the SEI layer also forms on the cathode, but this is much less well characterised.

There are many financial benefits if the total formation and conditioning time can be reduced.[19] Storing cells during conditioning costs money, for buildings, heating, staff time, and invested working capital. However, the cell chemistry must be stable at the end of conditioning, to allow effective screening, and ensure compliance with safety and abuse tests. Also, an accelerated conditioning protocol may compromise the long term performance of the cell.

This paper investigates formation and conditioning, in a commercial EV cell chemistry. The cells contain a graphite anode, and a mixed cathode with $LiMn_2O_4$ and a layered metal oxide, with a proprietary electrolyte supplied by our industrial partner, which includes sulfur and boron containing additives.[20] Electrodes from the dry pouch cell were used to construct coin cells, and test different formation and conditioning protocols. The three key parameters were duration, temperature and state of charge:

- The total duration of the conditioning process requires optimisation. Overly long cell conditioning carries a financial penalty, so the time must be minimised, whilst still ensuring that the cell chemistry has stabilised. Here we study several conditioning protocols which involve two steps at different temperatures. Stage 1 at 45 °C for 6, 12 or 18 days was followed by stage 2 at 25 °C, for 1, 2 or 3 days.
- Temperature is an important factor in every chemical reaction, and it influences many aspects of lithium-ion cell behaviour. Here we study three different temperatures for formation and conditioning (5, 25 and 45 °C) utilising the 12 + 2 day conditioning protocol.
- Degradation reactions in lithium-ion batteries often depend on state of charge. Some of the degradation mechanisms are likely to be similar to the reactions occurring during operational ageing, and they commonly lead to increases in the interface layer thickness. Therefore, we have investigated the effect of state of charge at 25%, 50% and 75% during the conditioning process.

There is a significant excess of electrolyte in coin cells, in comparison to fully engineered cells. Therefore, it is unrealistic to study filling protocols in anything but the full sized cell. However, uniform wetting of the complete cell is an important part of the overall formation and conditioning process. The

Table 1. Reactions that produce the SEI layer.

	Reactants		Products
1	RO.CO.OR′ + 2 Li^+ + 2 e^-	→	ROLi (s) + R′OLi (s) + CO (g)
2	RO.CO.OR′ + 2 Li^+ + 2 e^-	→	Li_2CO_3 (s) + R.R′ (g)
3	2 $C_3H_4O_3$ + 2 Li^+ + 2 e^-	→	LiO.$C_4H_4O_4$.OLi (s) + C_2H_4 (g)
4	$LiPF_6$	→	LiF (s) + PF_5
5	PF_5 + H_2O	→	POF_3 + 2 HF
6	PF_5 + n Li^+ + n e^-	→	LiF (s) + Li_xPF_y
7	POF_3 + n Li^+ + n e^-	→	LiF (s) + $Li_xPO_yF_z$
8	n VC	→	poly (VC)
9	HF + ROLi (s)	→	LiF (s) + ROH
10	2 HF + Li_2CO_3 (s)	→	2 LiF (s) + H_2O + CO_2 (g)
11	H_2O + Li^+ + e^-	→	LiOH (s) + $^1/_2$ H_2 (g)
12	LiOH (s) + Li^+ + e^-	→	Li_2O (s) + $^1/_2$ H_2 (g)

wetting of the electrodes by liquid electrolyte has been investigated in a combined experimental and modelling approach.[21] There was good correlation between wetting rates and properties of the electrolyte e.g. the ratio of surface tension to viscosity. Further experiments showed the influence of temperature, electrode porosity, and the solvent used to coat the electrodes.[22] Unfortunately, there is a big difference in complexity between the wetting of a 20×20 mm electrode token and a complete 30 A h pouch cell. Gas bubbles and pockets remaining within full sized cells can be detected with ultrasonic scanning[23] and neutron radiography.[24]

Changes in electrochemical performance (impedance, capacity and capacity fade) were correlated with different formation and conditioning protocols. The most beneficial parameters from the temperature, state of charge and duration experiments were then combined, to further optimise the conditions. The test sequence for the electrochemical tests is set out in Figure 1.

Surface analysis was carried out at the extremes of the temperatures investigated, 5 °C and 45 °C, giving the elemental composition of the SEI. Initial experiments revealed the presence of both sulfur and boron, in anodes that had been exposed to electrolyte, which were not present in the original (dry) coating. The (proprietary) electrolyte includes one or more additives, containing sulfur and boron. The most likely identity of the additives are LiBOB (lithium bis oxalate borate) and propane sultone.[25]

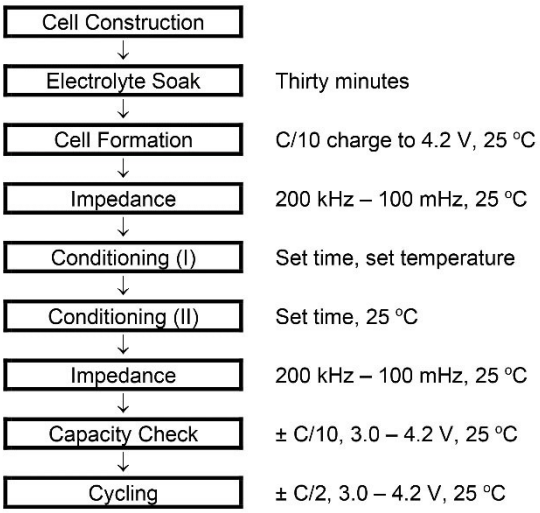

Figure 1. Formation and conditioning process schematic.

Table 2. Test protocols with different conditioning durations.

Protocol stage	Temperature [°C]	Conditioning duration [days] D1	D2	D3
Conditioning (I)	45	6	12	18
Conditioning (II)	25	1	2	3

2. Results and Discussion

2.1. Duration

Table 2 shows three protocols evaluated in this work; all the cells were formed at 25 °C. The two temperature conditioning protocol was derived from the current manufacturing protocol for this cell chemistry. A high discharge capacity after conditioning and low capacity fade on cycling are indicative of a successful conditioning protocols. Figure 2 shows capacity vs. cycle life following conditioning, for three different durations (highest capacity of three cells). D1 which had been conditioned for 7 days, showed higher capacity but higher fade rates than D2 and D3, which were conditioned for 14 and 21 days respectively. The fade rates are shown by comparing the discharge capacities on cycle fifty to cycle five, as shown in Figure 3A. The longer protocols D2 and D3 gave similar results, indicating that seven days conditioning is not enough, but fourteen days are comparable to twenty one days.

Impedance measurements were taken at the end of formation, and at the end of conditioning. In all cases, both the series and electrochemical impedances increased after conditioning. Figure 4 shows results, for three coin cells conditioned for 18+3 days (D3 protocol). The spectra showed increases in both the series and electrochemical resistances. The resistance values were obtained by fitting the data to a simple equivalent circuit model. The results are plotted in Figure S1A and S2A. There was some scatter, but no specific trend associated with any of the protocols.

2.2. Temperature

Table 3 shows the matrix of different formation and conditioning (I) protocols at 5, 25 and 45 °C. The conditioning protocol was chosen from the duration study as 12+2 days; all of the conditioning (II) steps were at 25 °C. Figure 3B plots the discharge capacities after five and fifty cycles. The series and electrochemical resistances are in Figure S1B and S2B.

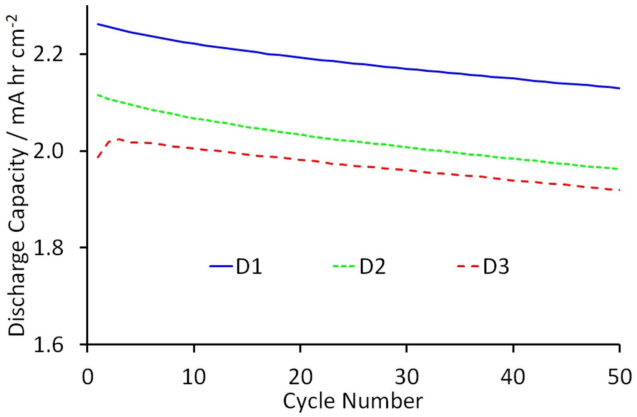

Figure 2. Typical discharge capacities during characterisation cycles after conditioning.

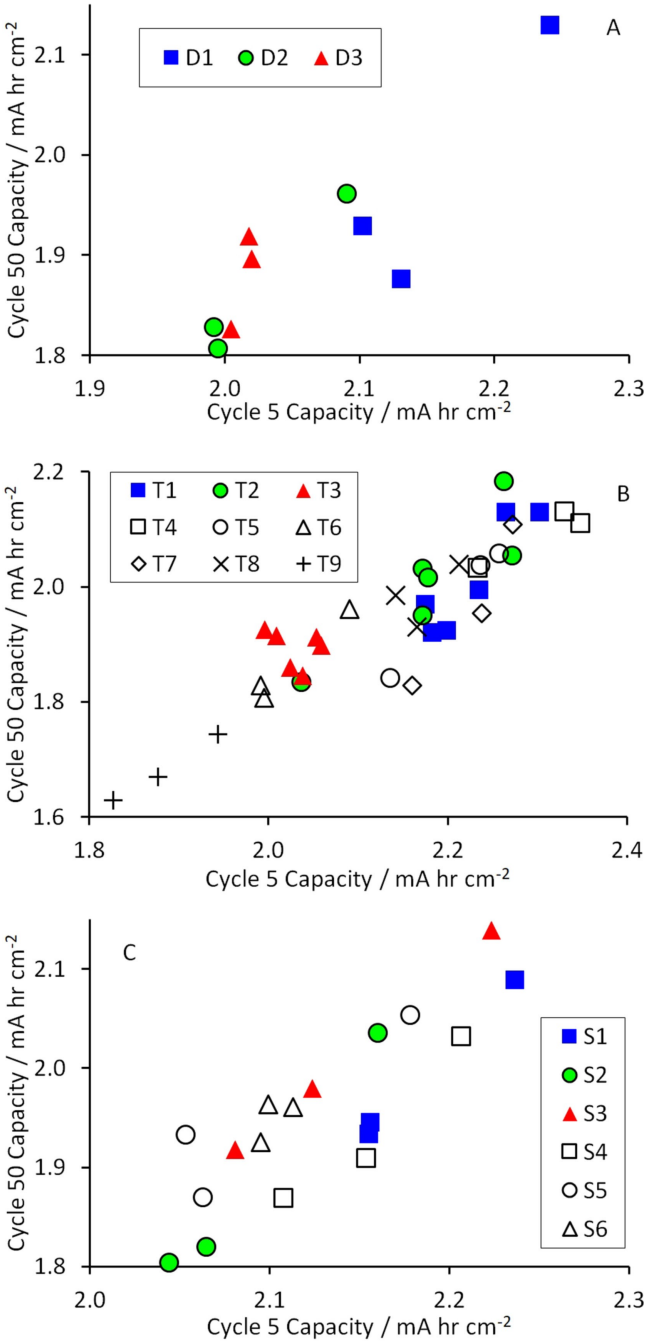

Figure 3. Effect of test protocols for a) conditioning duration, b) formation and conditioning temperature and c) state of charge on capacity retention over fifty cycles.

The lowest capacities observed (T6 and T9) followed conditioning at 45 °C, following formation at 25 °C or 45 °C. In comparison T3, forming at 5 °C followed by conditioning at 45 °C, had average capacities and relatively high capacity retention. Arguably the best protocol was T4, with formation at 25 °C followed by conditioning at 5 °C. The trend for all of the cells formed at 5 °C was similar; capacity retention during cycling was much better for cell conditioning at 45 °C than at 25 °C or 5 °C. Overall, the most promising protocol for further

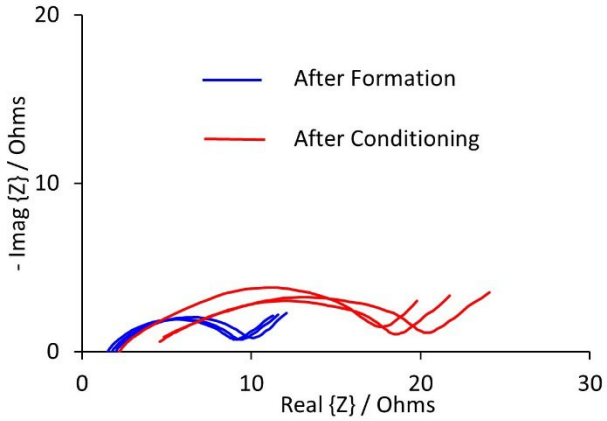

Figure 4. Typical impedance spectra before and after conditioning.

Table 3. Test protocols with different formation and conditioning temperatures.

Formation temperature [°C]	Conditioning (I) temperature [°C] 5	25	45
5	T1	T2	T3
25	T4	T5	T6
45	T7	T8	T9

investigation was considered to be T4 (formation at 25 °C, conditioning at 5 °C).

2.3. State of Charge

Table 4 shows the protocols that were involved; all of them used formation at 25 °C, twelve days of conditioning at 45 °C, and then two days of conditioning at 25 °C. For protocols S1, S2 and S3, a partial charge was used. For the other three protocols, a full charge was followed by a partial discharge. The cell voltages for S1, S2, S3 and D2, during formation and the capacity check after conditioning, are shown in Figure S3. The curves shown were for the median of three, nominally equivalent cells. It was evident that state of charge had an impact in particular upon first cycle loss.

The capacities after five and fifty cycles are plotted in Figure 3C. The cells conditioned at 25% SoC (S1 and S4) showed lower capacity retention than the other cells. The most consistent results were for protocol S6, with conditioning at 75% SoC following a full charge. Impedance spectra for lithium-ion cells usually change with state of charge. The cells conditioned at 25% SoC (S1 and S4) had relatively large

Table 4. Test protocols using different states of charge during conditioning.

Protocol type	State of charge during conditioning [%] 25	50	75
Partial charge	S1	S2	S3
Full charge + Partial discharge	S4	S5	S6

electrochemical resistances, both before and after conditioning, as shown in Figure S1C and S2C. Measurements in three electrode cells showed that the anode voltage was ~0.2 V vs. Li/Li^+ at 25% SoC, and ~0.1 V vs. Li/Li^+ at 50% SoC. Therefore, the electrochemical reactions that form the initial SEI layer on the anode would have been complete, even at 25% SoC.

2.4. Combined Protocols

Two of the most promising protocols from the previous sections were T4 (formation at 25 °C, conditioning at 5 °C), and S6 (conditioning at 75% SoC). Therefore different conditioning times for T4, and different conditioning temperatures for S6 were investigated. The protocols set out in Table 5 were used for further tests. The initial results with S7 were very promising, so the conditioning time was also varied as shown in protocols S9 and S10. The same testing regime was used for these additional protocols. Figure 5A shows the effects of low temperature conditioning duration. The cells tested on the shorter T10 protocol showed high variability. One of the cells with high capacity retention exhibited an increasing capacity over the first ten cycles. However, the resistance values obtained from the impedance measurements, plotted in Figures S4A and S5A, showed very little variation, particularly the electrochemical resistances. No improvement was noted over T4.

The results with formation at 75% SoC are plotted in Figure 5B. The best results were achieved with conditioning at 25 °C. Shortening or extending the conditioning time in protocols S9 and S10 was not beneficial. The resistance values are collected in Figures S4B and S5B. There was more spread in the series resistance values, and the highest electrochemical resistances were for conditioning at 45 °C.

Table 5. Combination test protocols.

Protocol I. D.	Duration [days]	Conditioning (I) [°C]	SoC [%]
T10	6+1	5	100
T4	12+2	5	100
T11	18+3	5	100
S6	12+2	45	75
S7	12+2	25	75
S8	12+2	5	75
S9	6+1	25	75
S10	18+3	25	75

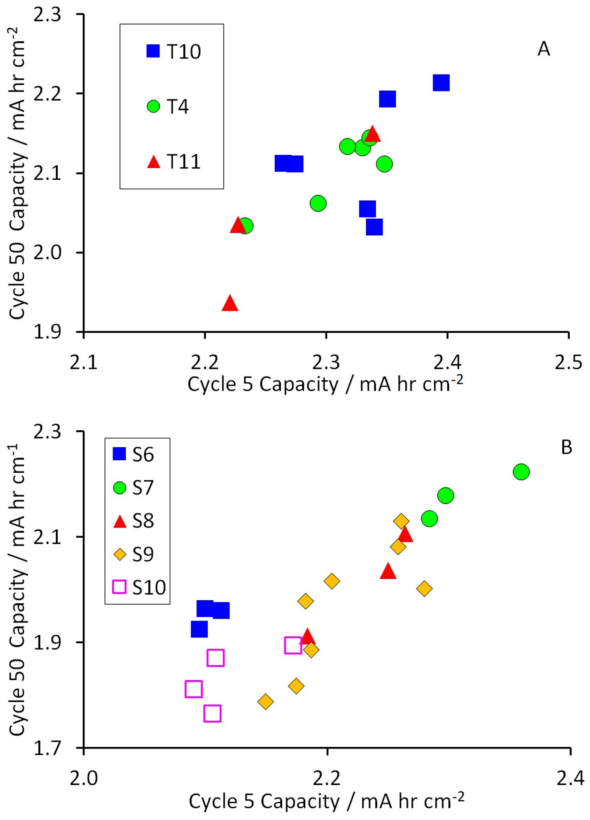

Figure 5. Effect of combined protocols involving a) temperature and b) state of charge on capacity retention over fifty cycles.

2.5. XPS Spectroscopic Results

Two sets of cells were formed at 25 °C, and then conditioned at either 5 °C or 45 °C. Cells were disassembled after different conditioning durations, and the anodes were examined using XPS spectroscopy. Some representative spectra for the elements detected are shown in Figure 6. The atomic% for each element are then plotted against conditioning duration in Figure 7. The labels 19+X imply 19 days at the set temperature, and then X days at 25 °C. This was based on the conditioning protocol from the industrial cell manufacturer.

All the **lithium** 1s samples contained a peak in the 55–56 eV range. The cells conditioned at 45 °C also produced a second peak, at a slightly lower binding energy. It can be difficult to resolve peaks from lithium fluoride (~55.6 eV) and lithium carbonate (~55.2 eV) in lithium 1s spectra; most lithium compounds produce peaks at around 55.5 eV.[26] Both LiF and Li_2CO_3 are expected to be present in the SEI layer. The samples were taken from charged cells i.e. with lithiated graphite anodes. Therefore, the second peak found in the sputtered samples could be this lithium. Li_xC_6 is listed at both 54.5 eV[27] and 57.6 eV.[28] Alternatively, it could also be Li_2O from argon sputtering of Li_2CO_3, although Li_2O is listed at 55.5 eV[26] and 53.7 eV.[29] Over the course of the conditioning period, there was a slight decrease in the lithium at% at 5 °C, and a roughly stable at% at 45 °C. It was noticeable that the lower energy peak was only detected for storage at the higher temperature.

The presence of **boron** in the XPS measurements was initially unexpected. Most of the spectra contained just one peak at around 191 eV, but up to three peaks could be present. There are many boron compounds with B 1s binding energies in the 192–193 eV range, for example B_2O_3, H_3BO_3, $Na_2B_4O_7$.[26] The lithium salts LiBOB and $LiBF_4$ give peaks at 194 eV and 195.5 eV respectively.[30] Following analogous reduction pathways to $LiPF_6$, $LiBF_4$ is expected to produce Li_xBF_y and $Li_xBO_yF_z$, with peaks at ~197 eV and ~194 eV, again respectively.[31] After sputtering, the $Li_xBO_yF_z$ peak was broader, with a lower peak

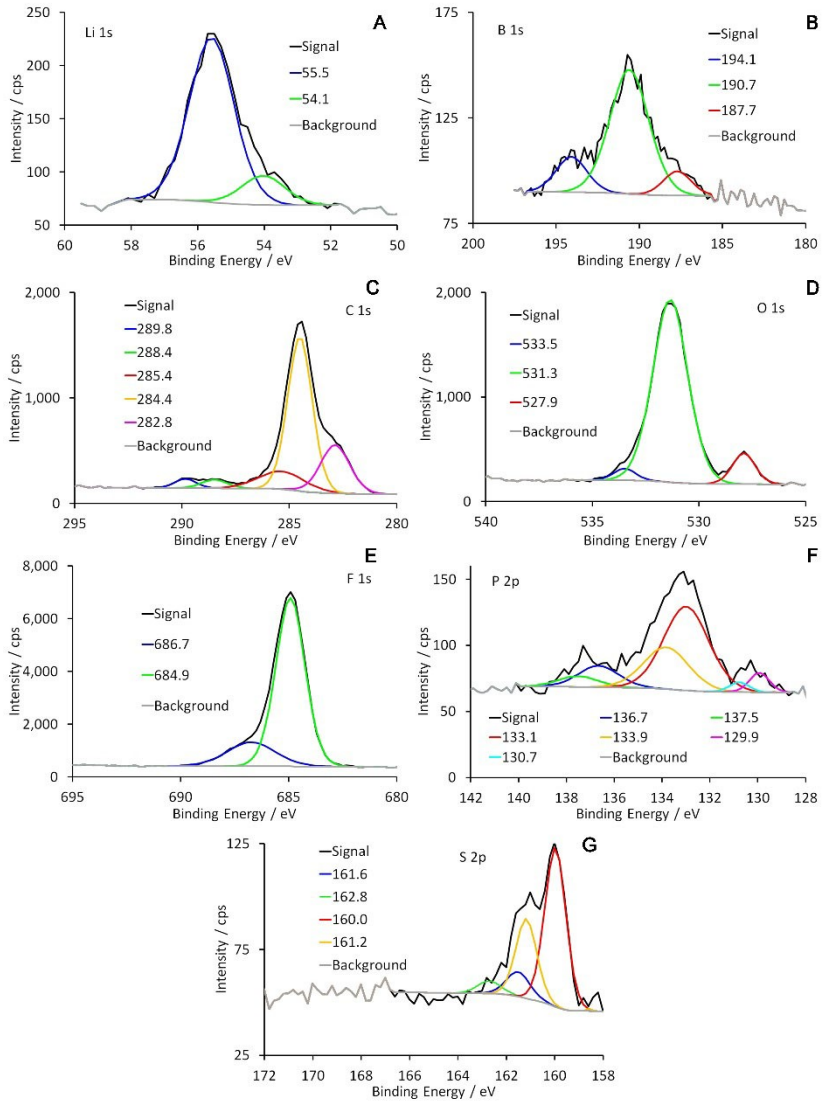

Figure 6. Typical spectra obtained using XPS spectroscopy: a) lithium, b) boron, c) carbon, d) oxygen, e) fluorine, f) phosphorous, g) sulfur.

energy, indicating the creation of a greater variety of oxygenated boron states.[31] It is more likely that the boron containing additive was actually LiBOB. Reduction mechanisms have also been proposed for LiBOB.[32] By analogy with various mechanisms proposed for ethylene carbonate (EC), the initial reaction produces a dimerization with EC. A further reduction step gives a polymer with an oxygen–boron chain, and various side products:

$$\mathbf{B1}: \ LiB(C_2O_4)_2 + C_3H_4O_3 + Li^+ + e^- \rightarrow LiO.CO.CO.O.CH_2.CH_2.O.CO.O.B(C_2O_4)Li$$

$$\mathbf{B2}: \ LiB(C_2O_4)_2 + C_3H_4O_3 + 2\ Li^+ + 2\ e^- \rightarrow [O.B(C_2O_4)Li]_n + Li_2C_2O_4 + CO_2\ (g) + C_2H_4\ (g)$$

The main peak is likely to be one of these oxygen–boron compounds, and the 194 eV peak is LiBOB itself. The lower energy peak at ~187 eV, seen in one sample, is in the energy range for a boride or borohydride. Overall, the boron content increased with conditioning time at both temperatures, and it was consistently higher during conditioning at 45 °C. In theory, the samples after zero storage duration should be identical. In practice, there were variations in at% for almost all the elements.

The **carbon** 1s spectra contained the greatest number of peaks. As with lithium, there are some variations in the reported peak energies for different carbon compounds. A typical set of energy values is; graphite (284.4 eV), hydrocarbons (285.0 eV), alcohols and ethers (286.2 eV), carbonyls (287.6 eV), carboxylic acids and esters (288.8 eV) and carbonates (290.6 eV).[33] If vinylene carbonate is present in the electrolyte, then poly (VC) can give a higher energy peak, at about 291.5 eV.[34] The lower energy peak at around 282 eV would normally be interpreted as a carbide, and in this case, therefore, lithiated carbon.

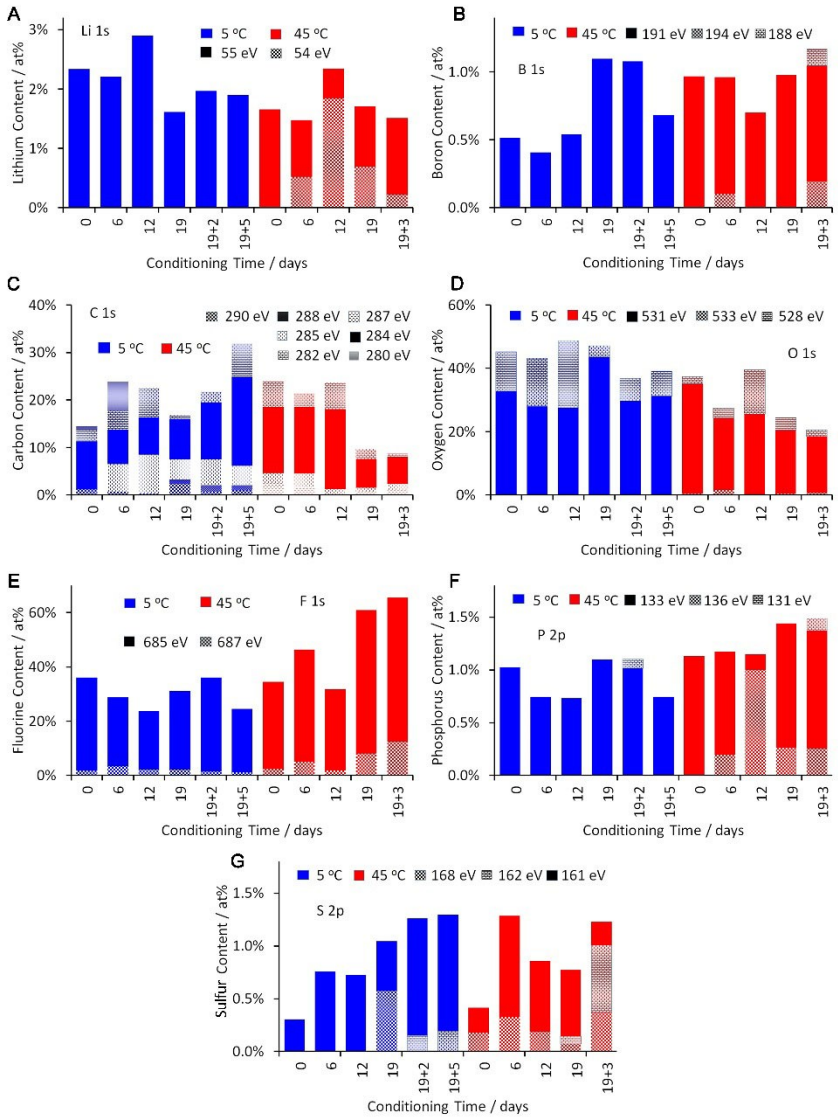

Figure 7. Changes during conditioning for each element from XPS results: a) lithium, b) boron, c) carbon, d) oxygen, e) fluorine, f) phosphorous, g) sulfur.

Experimental measurements have produced a peak at 282.5 eV,[35] though calculations predicted a peak energy of 283.6 eV for LiC_6.[27] The peak at around 280 eV is below the normal energy range for carbides, but there are no other obvious peak energies in this region. The carbon spectra were by far the most complicated and difficult to interpret. The trends in at% were clear, with a steady increase at 5 °C, and a steady decrease at 45 °C. The main changes were associated with the peak attributed to graphite, at 284.4 eV. Most of the samples contained a carbonate peak at 290 eV, and all of them contained a carbide peak at ~282 eV. The 45 °C samples had peaks in the 286–287 eV range, attributed to alcohols or ethers. At 5 °C, the hydrocarbon peak at 285 eV obscured this region. A different deconvolution algorithm might have produced a different fitting. At 5 °C, there was an emerging carbonyl peak at 288 eV; at 45 °C this would have been masked by the carbonate peak.

Most of the **oxygen** 1s spectra contained two peaks, but some also had a third peak. The main peak was due to C=O double bonds, at 531–532 eV. The higher energy peak was for C–O single bonds, at 533–534 eV.[34] The lower energy peak is likely to be Li_2O, in the range of metal oxides.

Unfortunately, Li_2O can be produced by the argon sputtering of Li_2CO_3,[16] as an artefact of measurement, rather than a genuine component. The oxygen content decreased slightly at 5 °C, and more significantly at 45 °C. There was no detectable C–O single bond oxygen at 5 °C, and very little at 45 °C. This suggested that there was a very limited amount of lithium alkoxide (ROLi) in the SEI layer, at any stage.

The **fluorine** spectra consistently produced two peaks at the same energy values. The main peak at around 685 eV was LiF.[30] There are a number of possible contributors to the higher energy peak at around 688 eV, including $LiPF_6$, PVDF, Li_xPF_y and $Li_xPO_yF_z$.[30,34,36] The progression of fluorine at% values showed a slight decrease at 5 °C, and a significant increase at

45 °C. If the higher energy peak was due to PVDF or $LiPF_6$, the peak area would not be expected to increase with conditioning time. However, contributions from Li_xPF_y and $Li_xPO_yF_z$ might be expected to change, and in this case at 45 °C, increase.

As explained in the experimental section, **phosphorus** 2p spectra contain doublets due to the different spin states. The experimental data was always fitted in pairs, with a $\Delta = 0.84$ eV. In published results, it is not always clear whether the results refer to just the 3/2 spin peak, or an average of both spins. Up to three doublets were observed. The main peak at 133–134 eV was attributed to $Li_xPO_yF_z$. The higher energy peak at 136–137 eV could be $LiPF_6$ or Li_xPF_y.[36] A surprising peak at ~131 eV was seen in two samples. This energy is typical of elemental phosphorus and organic compounds like $(C_6H_5)_3P$,[26] neither of which are expected to be present. There was no clear trend through the conditioning process at 5 °C, though no Li_xPF_y was detected. At 45 °C, there was more phosphorus, and the at% increased during conditioning. The sample from twelve days at 45 °C showed an atypical distribution of energies, and indeed most of the results from this sample did not follow the general trend. However, a repeat XPS measurement gave very similar results.

There are a limited number of published results for **sulfur** compounds in SEI layers. A typical spectrum contained four peaks, in two doublets. Again, the 3/2 and 1/2 spin peaks were fitted separately, with a $\Delta = 1.2$ eV. Peaks at 168 eV are sulfates or sulfones, whereas peaks at 161 eV are sulfides.[26] The attribution and reaction mechanisms for possible sulfur compounds are discussed in greater detail in a separate publication.[37] Since compounds like $CH_3.S.CH_3$ are liquid at room temperature, it seems more likely that the sulfide compounds present are Li_2S (160.5/161.7 eV) and CH_3SLi (162.1/163.3 eV). At 5 °C, there was a steady increase in sulfur content throughout conditioning, while at 45 °C, the main increase occurred by day six. The peak at 162 eV only appeared towards the end of conditioning, so it is possible that it was produced by a conversion reaction like:

S1: $Li_2S + CH_3OLi \rightarrow CH_3SLi + Li_2O$

S2: $Li_2S + CH_3OH \rightarrow CH_3SLi + LiOH$

2.6. Discussion

It is clear that the formation and conditioning protocol has a significant impact on the performance of lithium-ion cells. Typically higher temperatures have been used in conditioning protocols. In this work, we have observed that for formation at 25 °C and up to 100% SoC, the cells that were conditioned at 5 °C performed better, with higher capacities and longer lifetimes, than those that were mainly conditioned at 45 °C. The results showed that the SoC during conditioning was also important. There was a significant spread in the results, but from this study, the cells conditioned at 50% SoC had greater capacity fade than those at 25% or 75% SoC. To reduce the total time for formation, a 7 day protocol was investigated and compared to two and three week protocols. The deviation in the cell batches at 7 days was large. However, comparing two and three week conditioning, the differences were less than the natural cell to cell variation between nominally equivalent cells. Thus, it is possible to establish a two week conditioning protocol for this cell chemistry, and reduce this from a three week conditioning protocol.

The XPS results for cells conditioned at 5 °C and 45 °C showed differences between the two temperatures, and changes in the SEI composition with conditioning duration. The three major components detected in the spectra were carbon, oxygen and fluorine. At 5 °C, the carbon at% increased during conditioning, while the oxygen and fluorine at% decreased. At 45 °C, the fluorine at% increased significantly, and the carbon and oxygen at% decreased. This could be due to the conversion of lithium carbonate to lithium fluoride, due to trace HF in the electrolyte. However, the main carbon species that disappeared was the graphite peak at 284.4 eV, indicating the deposition of extra lithium fluoride.

At 5 °C, the formation of the interface appears more complicated. Lithium fluoride is usually the end point of SEI formation reactions. Therefore, a decrease in fluorine at% implies an increase in some other component, rather than a loss of LiF. The increase in graphite content implies a thinning of the SEI layer, either by selective dissolution, or by dissolution/re-precipitation in a denser, less porous form.

The other four elements present were lithium, boron, phosphorus and sulfur. XPS measurements on the lithium salts $LiPF_6$ and LiBOB showed that the atomic% values were relative, rather than fully quantitative, despite the scaling factor used in data analysis. The lithium at% was around 5% of the expected value, and the phosphorus at% was around 25%, but the boron at% was pretty much 100%. Thus, there was more phosphorus and a lot more lithium in the samples than the atomic% values suggested.

There was a slight decline in the lithium at% through conditioning at 5 °C. If the SEI layer densifies at this temperature, then the increased graphite signal will reduce the lithium at%. At 45 °C, the lithium at% was roughly constant, implying that any growth in the SEI layer involved lithium containing compounds. The boron spectra are difficult to interpret, partly because boron in SEI layers is much less widely studied than the other elements discussed here. Changes in the oxygen : boron ratio will change the peak energy slightly, but there is no guarantee that different peaks can be resolved.

The phosphorus at% showed no clear cut trend at 5 °C. At 45 °C, there was in an increase in both the Li_xPF_y and $Li_xPO_yF_z$ signals, with conditioning time. Some of the increase in fluorine content was therefore associated with these compounds, and not just LiF. The reaction mechanisms proposed for the creation of these two compounds in the SEI layer involve the electrochemical reduction of PF_5 and POF_3, respectively. In the absence of a (net) electrical current, the most likely reducing agent was lithium intercalated into graphite. The cell capacity

was lower after conditioning at 45 °C, compared to 5 °C, implying increased resistance or loss of active lithium (or both). The reactions that increase the Li_xPF_y and $Li_xPO_yF_z$ content would consume active lithium. The sulfur at% increased, in general terms, at both 5 °C and 45 °C. The main components were sulfides, rather than sulfates. It is easier to explain the presence of sulfide peaks if the additive in the electrolyte was propane 1,3 sultone, rather than propene 1,3 sultone.[37]

3. Conclusions

This work highlights the importance of formation and conditioning protocols for good electrochemical performances of lithium-ion batteries. The commercial graphite vs. mixed oxide cathode chemistry exhibited marked differences in capacity and cycle life retention depending upon the protocols investigated.

There was a significant improvement on the initial base level protocol of formation at 25 °C to 100% state of charge, followed by conditioning at 45 °C. In tests varying a single key control parameter, the most important findings were:

- Duration: One week was insufficient as a total conditioning time, but two weeks and longer showed similar electrochemical performances.
- Temperature: Conditioning at 5 °C gave higher cell capacities than conditioning at 45 °C, and comparable capacity retention. However, after formation at 5 °C, conditioning at 45 °C gave the best capacity retention.
- State of charge: The best cell performance was achieved with conditioning at 75% state of charge, reached by a full charge and then a 25% discharge

In tests of combined protocols, conditioning at 75% SoC and 25 °C gave the highest initial capacity and good capacity retention, with two weeks the optimum conditioning duration.

The surface analysis from the anodes from cells conditioned at either 5 °C or 45 °C, showed chemical rearrangement of the surface electrolyte interface layer during the conditioning step. The SEI layer during conditioning at 5 °C was denser and thinner, giving a stronger graphite signal from the active material, and less oxygen and fluorine. The SEI layer during conditioning at 45 °C appeared thicker, diminishing the graphite signal. At this temperature, there were increases in the phosphorus and particularly the fluorine content, as conditioning progressed.

This work shows that there is significant further scope for improvement of the stability of the interface layers for a high capacity and low capacity fade rate for lithium-ion batteries. The conditioning process that follows the formation charge involves changes in the SEI chemical composition, and is still not fully understood. This study gives insights into the conditions required for optimised cell performances.

Experimental Section

The anode, cathode and separator sheets were extracted from an unfilled pouch cell, used in a commercial EV battery. The electrode coatings were double sided, and had to be converted to single sided before use. This was achieved using a minimum quantity of NMP (n-methyl pyrrolidone) and gentle scraping. After cutting and vacuum drying, electrode disks were used to make 2032 coin cells. The separator and electrolyte were from the original pouch cell. The proprietary electrolyte contained $LiPF_6$, ethylene carbonate, propylene carbonate and diethyl carbonate.

The cells were constructed in a dry room, with a dew point of less than −40 °C. During formation and cycling, a CC-CV protocol was used, with the constant voltage step terminated when the current had dropped to a tenth of the constant current value. After conditioning had completed, the cells were charged and then discharged (both C/10), before the start of the fifty cycles. All the cycling tests used a Maccor 4000 series unit, apart from the formation half cycles at 5 °C and 45 °C, which used a Bio Logic BCS-805 cycler. The cells for XPS measurements were formed at C/10 and 25 °C, and then conditioned at either 5 °C or 45 °C.

The impedance measurements used a Bio Logic VMP3, operated in potentiostatic mode with a 10 mV perturbation. The spectra were fitted to an equivalent circuit containing a series resistance, a resistor//CPE parallel combination and another constant phase element for the low frequency tail. Most of the spectra contained only one semi-circle, which was attributed to the "electrochemical" resistance. This encompassed the charge transfer and film resistances at both the anode and the cathode.

Cells were disassembled in an argon filled glove box. All the XPS measurements reported here were on anode samples, but both electrodes were recovered. To avoid dissolving any SEI components of interest, the samples were not rinsed in DMC.[30] The samples were transported from the glove box to the spectrometer using an air and water tight transfer vessel. The XPS measurements were made on a Kratos AXIS Ultra DLC spectrometer. After sample transfer, the measurement chamber was pumped down to a very low vacuum. Following an initial measurement, the samples were sputtered in argon for ten minutes, to remove any residues from electrolyte evaporation, and then by a repeat measurement. It should be noted that sputtering can decompose SEI components, for example, converting lithium carbonate to lithium oxide.[29] Data was exported from the spectrometer, and analysed using Casa XPS software. For each elements, peaks were added and fitted, until the error between the experimental and fitted intensities was sufficiently low. Each peak had a standard Gaussian shape. For phosphorus and sulfur, the 2p elements can have either 3/2 or 1/2 spin states, which leads to a doublet in the XPS spectrum. During the fitting process, a defined energy gap of 0.84 eV (P) or 1.2 eV (S) was imposed. The 3/2 peak was required to be twice the area of the 1/2 peak, and the FWHM (full width at half maximum) values were the same for both peaks.

Acknowledgements

WMG would like to acknowledge funding from the Advanced Propulsion Centre (APC), as part of the High Energy Density Battery project, and contributions from the other project partners, especially Nissan Motors (UK) Ltd. Also Professor David Greenwood, as WMG principal investigator, for his guidance and support, and to Dr. Marc Walker, Department of Physics, for his help with the XPS measurements.

Conflict of Interest

The authors declare no conflict of interest.

Keywords: ageing · conditioning · lithium-ion battery manufacturing · SEI

[1] S. J. An, J. Li, C. Daniel, D. Mohanty, S. Nagpure, D. L. Wood, *Carbon* **2016**, *105*, 52–76.
[2] C. Huang, K. Huang, H. Wang, S. Liu, Y. Zeng, *J. Sol. St. Electrochem.* **2011**, *15*, 1987–1995.
[3] F. German, A. Hintennach, A. LaCroix, D. Thiemig, S. Oswald, F. Scheiba, M. J. Hoffman, H. Ehrenberg, *J. Power Sources* **2014**, *264*, 100–107.
[4] P.-C. J. Chiang, M.-S. Wu, J.-C. Lin, *Electrochem. Solid-State Lett.* **2005**, *8*, A423–427.
[5] S. J. An, J. Li, Z. Du, C. Daniel, D. L. Wood III, *J. Power Sources* **2017**, *342*, 846–852.
[6] D. L. Wood III, J. Li, S. J. An, *Joule* **2019**, *3*, 2884–2888.
[7] T. S. Pathan, M. Rashid, M. Walker, W. D. Widanage, E. Kendrick, *J. Phys. E*, **2019**, *1*, 044003.
[8] C. Mao, S. J. An, H. M. Meyer, J. Li, M. Wood, R. E. Ruther, D. L. Wood III, *J. Power Sources* **2018**, *402*, 107–115.
[9] B. K. Antonopoulos, C. Stock, F. Maglia, H. E. Hoster, *Electrochim. Acta*, **2018**, *269*, 331–339.
[10] V. A. Agurba, J. W. Fergus, *J. Power Sources* **2014**, *268*, 153–162.
[11] P. Verma, P. Maire, P. Novák, *Electrochim. Acta* **2010**, *55*, 6332–6341.
[12] D. Aurbach, *J. Power Sources* **2000**, *89*, 206–218.
[13] Y. P. Stenzel, F. Horsthemke, M. Winter, S. Nowak *Separations* **2019**, *6*, 6020026.
[14] D. Aurbach, B. Markovsky, I. Weissman, E. Levi, Y. Ein-Eli, *Electrochim. Acta* **1999**, *45*, 67–86.
[15] P. Lu, C. Li, E. W. Schneider, S. J. Harris, *J. Phys. Chem. C*, **2014**, *118*, 896–903.
[16] H. Bryngelsson, M. Stjerndahl, T. Gustafsson, K. Edström, *J. Power Sources* **2007**, *174*, 970–975.
[17] L. Wang, A. Menakath, F. Han, Y. Wang, P. V. Zavalij, K. J. Gaskell, O. Borodin, D. Iuga, S. P. Brown, C. Wang, K. Xu, B. E. Eichhorn, *Nat. Chem.* **2019**, *11*, 789–796.
[18] J. Henschel, C. Peschel, S. Klein, F. Horstemke, M. Winter, S. Nowak, *Angew. Chem. Int. Ed.*, **2020**, *59*, 6128–6137.
[19] D. L. Wood III, J. Li, C. Daniel, *J. Power Sources* **2015**, *275*, 234–242.
[20] http://www.eco-aesc-lb.com/en/product/liion_ev/.
[21] A. Davoodabadi, J. Li, Y. Liang, D. L. Wood III, T. J. Singler, C. Jin, *J. Power Sources* **2019**, *424*, 193–203.
[22] A. Davoodabadi, J. Li, H. Zhou, D. L. Wood III, T. J. Singler, C. Jin, *J. Energy Storage* **2019**, *26*,101034.
[23] http://ultrangroup.com/applications/.
[24] J. B. Hadebank, F. J. Günter, N. Billot, R. Gilles, T. Neuwirth, G. Reinhart, M. F. Zaeh, *Int. J. Adv. Manu. Tech.* **2019**, *102*, 2769–2778.
[25] Japanese Patent 2012-243461A, H. Sasaki, T. Noguchi, NEC Corporation.
[26] J. F. Moulder, W. F. Stickle, P. E. Sobol, K. D. Bomben in *Handbook of X-ray Photoelectron Spectroscopy*, Perkin Elmer, **1992**.
[27] K. Kanamura, S. Shiraishi, H. Takezawa, Z. Takehara, *Chem. Mater.* **1997**, *9*, 1797–1804.
[28] V. Z. Mordkovich, *Synth. Met.* **1996**, *80*, 243–247.
[29] K. Edström, M. Herstedt, D. P. Abraham, *J. Power Sources* **2006**, *153*, 380–384.
[30] L. Somerville, J. Bareno, P. Jennings, A. McGordon, C. Lyness, I. Bloom, *Electrochim. Acta* **2016**, *206*, 70–76.
[31] M. Herstedt, H. Rensmo, H. Siegbahn, K. Edström, *Electrochim. Acta* **2004**, *49*, 2351–2359.
[32] A. Xiao, L. Yang, B. L. Lucht, S.-H. Kang, D. P. Abraham, *J. Electrochem. Soc.* **2009**, *156*, A318–327.
[33] R. I. R. Blyth, H. Buqa, F. P. Netzer, M. G. Ramsey, J. O. Besenhard, P. Golb, M. Winter, *Appl. Surf. Sci.* **2000**, *167*, 99–106.
[34] M. Nie, J. Demeaux, B. T. Young, D. R. Heskett, Y. Chen, A. Bose, J. C. Woicik, B. L. Lucht, *J. Electrochem. Soc. Interface* **2015**, *162*, A7008–7014.
[35] R. Yazami, *Electrochim. Acta* **1999**, *45*, 87–97.
[36] A. M. Andersson, D. P. Abraham, R. Haasch, S. MacLaren, J. Liu, K. Amine, *J. Electrochem. Soc.* **2002**, *149*, A1358–1369.
[37] M. J. Lain, I. Rubio Lopez, E. Kendrick, *Submitted for publication*.

Manuscript received: March 3, 2020
Revised manuscript received: April 21, 2020
Accepted manuscript online: April 24, 2020
Version of record online: May 18, 2020